Gradient dynamics formulations of thin film equations - part 1

Uwe Thiele

Cambridge, July 2013

ITN MULTIFLOW

Loughborough University

Dewetting of simple (polymeric) liquids– Phases

G. Reiter (since 1992)[1–3]

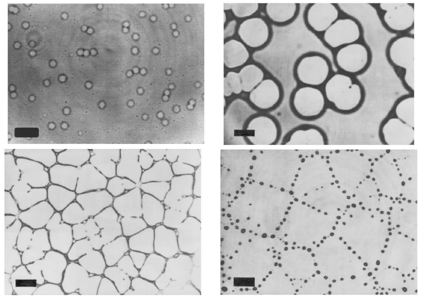

40 nm polystyrene films on silicon oxide (bar 100 micron)

Dewetting – Rupture mechanisms

J. Becker, G. Grün, R. Seemann, H. Mantz, K. Jacobs, K. R. Mecke, and R. Blossey (2003)[4]

Spinodal dewetting

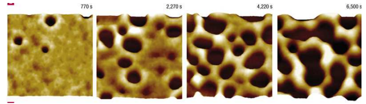

Heterogeneous nucleation

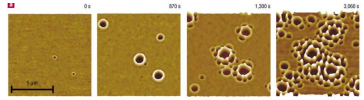

Ultrathin polystyrene films on silica (below 10 nm thickness)

Dielectric film in capacitor

Z. Lin, T. Kerle, T. P. Russell, E. Schäffer and U. Steiner (2002)[5]

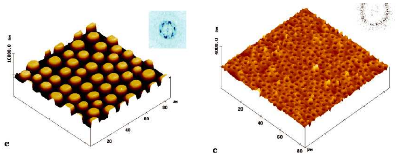

PS(550nm)/PDMS(700nm) and PS(730nm)/PMMA(290nm)

Can a simplified theory model the very slow coarsening?

Drop morphologies and stick-slip contact line motion

Podgorski, Flesselles and Limat (2001)[6]

Drop shape transformations

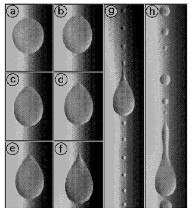

Schäffer and Wong (1998)[7]

Stick-slip motion of rising meniscus

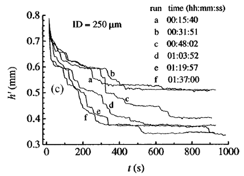

Can one predict the dynamics of the stick-slip motion for a depinning drop?

Front instabilities

G. Reiter and A. Sharma (2001)[8]

Dewetting: receding front

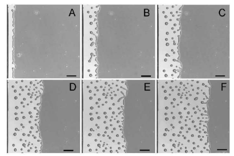

I. Veretennikov, A. Indeikina and H.-C. Chang (1998)[9]

Inclined plane: advancing front

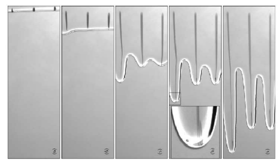

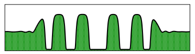

Drop on solid substrate - macroscopic equilibrium

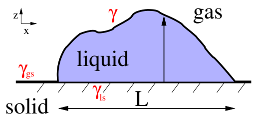

Interface energies (2d)

$$F_{macro} = \int_L (\gamma_{sl} + \xi\gamma)dx + \int_{D-L} \gamma_{sg}dx + \lambda\left[\int_L h dx - V\right]$$

$$ds = \xi dx = \sqrt{1 + \tfrac{1}{2}(\partial_x h)^2}dx$$

Minimisation: $\frac{\delta F_{macro}}{\delta h} = 0$

Euler-Lagrange equation

Laplace pressure

$-\gamma\kappa = \lambda = p = p_{in} - p_{out}$

Boundary conditions

Young-Laplace equation

$\gamma\cos\theta_e = \gamma_{sg} - \gamma_{sl}$

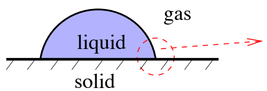

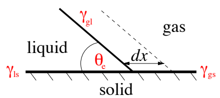

Mesoscopic equilibrium description

How to describe very thin films / contact regions ($h < 100$nm)?

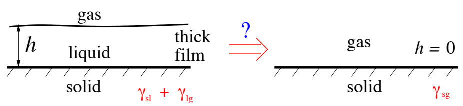

Young-Laplace-Derjaguin description $\gamma_{sl} + \gamma \longrightarrow \gamma_{sl} + \gamma + f(h)$

Interface Hamiltonian

$$F_{meso} = \int_A [\gamma_{sl} + \xi\gamma + f(h)]dA + \lambda\int_A (h - \bar{h})dA$$

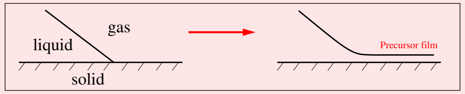

Wetting energy / Derjaguin (disjoining) pressure

$$\Pi(h) = -\frac{df(h)}{dh}$$

Example:

$$\Pi(h) = B\left[\frac{b}{h^3} - e^{-h/l}\right]$$

$b = A_{\mathrm{Ham}}/B$

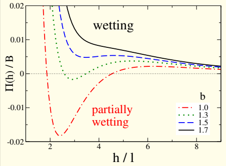

Microscopic origin

- Long-range van der Waals interaction ($h \lesssim 100\,\mathrm{nm}$) $\Pi(h) = A_{\mathrm{Ham}}/h^3$
- Short-range interactions (electric-double layer, entropic, hydration, $h \lesssim 10\,\mathrm{nm}$) $\Pi(h) = Be^{-h/l}$ or B/h^6

Theoretical approaches towards dynamics

Variational approach (purely energetic)
Equilibrium profiles and their stability
no dynamics, no most dangerous mode etc.
Blossey, Brinkmann, de Gennes, Dietrich, Lipowsky, Sekimoto, ...

(Navier)-Stokes with free surface
Gives the full picture of the purely hydrodynamic part
high computational effort, nearly no (semi)analytical results, contact line needs ad-hoc addition
Armstrong, Brown, Krishnamoorthy, Joo, Salamon, Thess, ...

(Navier)-Stokes plus phase-field
Avoids tracking of free surface
still tedious, tricky details (phase change, interface thickness)
Bestehorn, Jacqmin, Jasnow, McFadden, Pismen, Pomeau, Viñals

Long-wave (lubrication) approximation
Wetting properties, contact line motion, small surface slopes only (but arbitrary amplitudes), no short-scale structures
Benney, Davis, de Gennes, Reynolds, Ruckenstein, Sommerfeld, ...

Derivation of the film thickness evolution equation

(Navier-)Stokes and continuity equations plus boundary conditions
⇓
Scaling to obtain dimensionless equations
⇓
Long-wave scaling (introducing $\varepsilon = h/L = O(\theta_e)$)
⇓
Series expansion of all fields
⇓
Solving order by order in ε for velocity and pressure profiles
⇓
Use of continuity to obtain film thickness evolution equation

Evolution equation in long wave approximation (dim)

$$\partial_t h = -\nabla\cdot\{Q(h)\,\nabla\,[\gamma\Delta h + \kappa\Pi(h,x)] + \tilde{\mu}\,\mathbf{e}_x\}$$

$Q(h) = h^3/3\eta\ldots$ mobility factor
$\Delta h\ldots$ curvature pressure
$\mu\,\mathbf{e}_x\ldots$ driving
$f(h,x)\ldots$ local free energy

Examples of additional pressures $\Pi = -\partial_h f$

$\frac{b}{h^3} - \xi(x)\,e^{-h}$	antag. polar/apolar interaction
$-\frac{1}{h^3} + \frac{b}{h^6}$	long/short-range van der Waals
$b\xi(x)h - h^3$	Cahn-Hilliard equation
$\frac{3}{2}\,\mathrm{Bi\,Ma}\,\xi(x)\left[\log\left(\frac{h}{1+\mathrm{Bi}\,h}\right) + \frac{1}{1+\mathrm{Bi}\,h}\right] - h$	heated thin film
$\frac{\xi(x)}{[h+(d-h)\varepsilon]^2}$	electrostatic field

Evolution equations - linear nonequilibrium thermodynamics

Gradient dynamics on underlying energy functional $F[\phi]$

Single conserved order parameter field (Cahn-Hilliard-type)

$$\partial_t\phi = \nabla\cdot\left\{Q(\phi)\,\nabla\,\frac{\delta F[\phi]}{\delta\phi}\right\}$$

Single non-conserved order parameter field (Allen-Cahn-type)

$$\partial_t\phi = -Q_{\mathrm{nc}}(\phi)\frac{\delta F[\phi]}{\delta\phi}$$

Combinations possible

Horizontal substrate – dewetting simple liquid

Evolution equation for conserved order parameter field:
Film thickness

$$\partial_t h = \nabla\cdot\left\{Q(h)\,\nabla\,\frac{\delta F[h]}{\delta h}\right\}$$

with interface Hamiltonian (lyapunov functional)

$$F[h] \approx \int_A\left[\frac{\gamma}{2}|\nabla h|^2 + f(h)\right]\,dA$$

$f(h) = -\int\Pi dh\ldots$ wetting or adhesion energy
$Q(h) = h^3/3\eta\ldots$ mobility

Identical to
Long-wave hydrodynamics - film thickness evolution equation

$$\partial_t h = -\nabla\cdot\{Q(h)\,\nabla\,[\Delta h + \Pi(h)]\}$$

Nematic liquid crystal with strong antagonistic anchoring

Consistent film evolution equations from long-wave and variational approaches

$$\partial_t h = \nabla\cdot\left\{Q(h)\,\nabla\,\frac{\delta F[h]}{\delta h}\right\}$$

where

$$F[h] = \int_V\left[\frac{\gamma}{2}|\nabla h|^2 + \frac{K_{\mathrm{el}}}{2h^2}\right]\,dx$$

K_{el}=elastic constant of nematic liquid crystal (one constant approx) [cf. Cazabat et al. (2003) [10]]

Alternative:
Without 'elastic pressure' [S. Wilson & collab. (2007) [11]];
Opposite sign of 'elastic pressure' [Ben Amar & Cummings (2001) [12]]

T.-S. Lin et al., PoF, at press (2013)

Linear and nonlinear film stability - dewetting modes

Linear stability analysis

Ansatz:
$h(x,t) = h_0 + \varepsilon\exp(\beta t + ikx)$

Dispersion relation

$\beta = -k^2\,Q(h_0)\,(k^2 - k_c^2)$

with $k_c^2 = -\partial_{hh}f|_{h=h_0}$

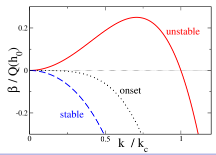

Stability diagram

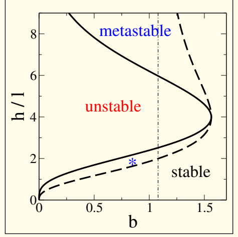

Bifurcation of steady drop states at $L_c = 2\pi/k_c$

Steady solutions – sitting drops and critical holes

Profiles

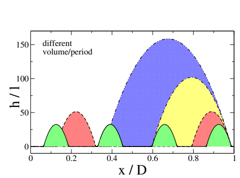

Families: Amplitude, Energy

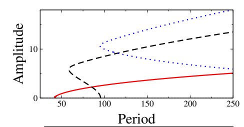

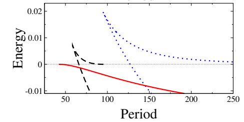

- supercritical bifurcation from the linearly unstable flat film (spinodal dewetting dominant)
- subcritical bifurcation from the linearly unstable flat film (nucleation may be dominant, secondary nucleation determines dynamics)
- flat film metastable: nucleation needed

Linear stability of steady solutions

Ansatz

$$h(x,y,t) = h_0(x) + \varepsilon\, h_1(x)\, \exp(iky + \beta t)$$

Gives linear eigenvalue problem for the growth rate β and disturbance h_1

$$\beta h_1(x) = \mathbf{S}[k, h_0(x)]\, h_1(x) \quad \text{with} \quad \mathbf{S}h_1 = N_0 h_1 + k^2 N_2 h_1 + k^4 N_4 h_1$$

$$\begin{aligned} N_0 h_1 &= -\{Q_h h_1\, [(h_{0xx} - f_h)_x]\}_x \\ &\quad -\{Q\,(h_{1xx} - f_{hh} h_1)_x\}_x \\ N_2 h_1 &= \{Q\, h_{1x}\}_x + Q\,(h_{1xx} - f_{hh} h_1) \\ N_4 h_1 &= -Q\, h_1 \end{aligned}$$

All derivatives of f are functions of $h_0(x)$.

Growth rates – critical defects vs. linear modes

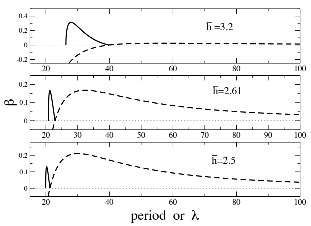

Defects dominate

Surface instability dominates

Film stability and rupture modes

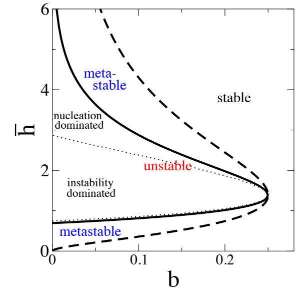

UT, M.G. Velarde and K. Neuffer, PRL 87, 016104 (2001); UT et al., PRE 64, 031602 (2001)

Short-time evolution - Profiles

Instability-dominated

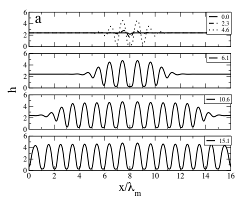

Nucleation-dominated

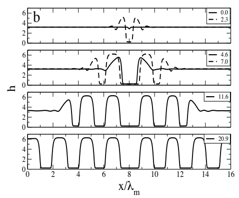

UT, M.G. Velarde and K. Neuffer, PRL 87, 016104 (2001); UT et al., ColSuA 206, 135–155 (2002)

Summary lecture 1

- Experiments with interface-dominated film/drop dynamics
- Modelling drops/films of simple liquids
- Long-wave expansion / gradient dynamics approach
- Analysis tools - illustrated for dewetting mechanisms

Gradient dynamics formulations of thin film equations - part 2

Uwe Thiele

Cambridge, July 2013

ITN MULTIFLOW

Loughborough University

Dewetting of two-layer films

M. Geoghegan and G. Krausch (2003)[13]

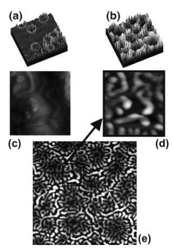

Dewetting PMMA (30nm) on PS (15nm)

A. Faldi, R. J. Composto, and K. I. Winey (1995)[14]

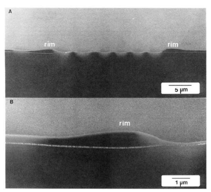

Polycarbonate on Polystyren-co-acrylonitril

Decomposition and dewetting

Wang & Composto (2003)[15], Geoghegan & Krausch (2003)[13]

Profile evolution

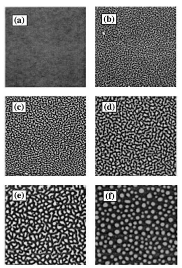

(a) $1\mu m \times 1\mu m$, (b-f) $10\mu m \times 10\mu m$

Schematics

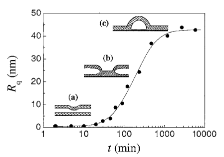

50 nm film of decomposing mixture of dPMMA and SAN

Experiment: More involved (Co-)Polymer blends/solutions

Flow-induced decomposition
Müller-Buschbaum *et al.* (2006)[16]

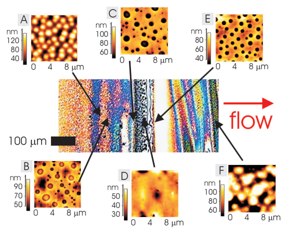

Chemical reaction – phase separation
Magerle et al.

Dewetting of suspensions - branched structures

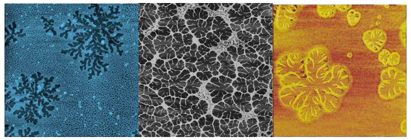

(a) Gold nanoparticles in toluene on silicon (Pauliac et al. 2008, $20\mu m \times 20\mu m$) [17]
(b) Aqueous collagen solution on graphite (Mertig et al. 1998, $5\mu m \times 5\mu m$) [18]
(c) Aqueous PAA solution on PS (Gu et al. 2002, $2.5\mu m \times 2.5\mu m$) [19]
(d) Kinetic Monte Carlo run of lattice gas model (Vancea et al. 2008 [20])

Deposition of line patterns from solutions/suspensions

Dewetting evaporating nanoparticle suspensions

Lin et al. (2007) [21]

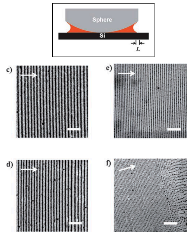

(CdSe/ZnS core/shell, 4.4nm, in toluene)
Conc: 0.25, 0.15, 0.05, 0.05mg/ml

Langmuir-Blodgett transfer of surfactants

Chi, Fuchs, Riegler et al. (1994,2004) [22,23]

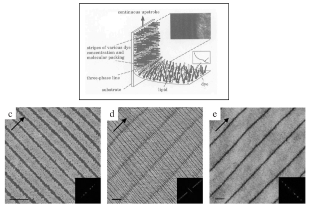

Transfer of DPPC onto silicon oxide
Transition with increasing lateral surface pressure
SFM images, bar $2\mu m$

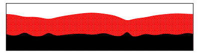

Two-layer film: evolution equations

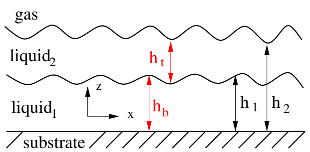

$$\frac{\partial h_b}{\partial t} = \nabla\left(Q_{bb}\nabla\frac{\delta F}{\delta h_b} + Q_{bt}\nabla\frac{\delta F}{\delta h_t}\right)$$
$$\frac{\partial h_t}{\partial t} = \nabla\left(Q_{tb}\nabla\frac{\delta F}{\delta h_b} + Q_{tt}\nabla\frac{\delta F}{\delta h_t}\right)$$

A. Pototsky, M. Bestehorn, D. Merkt and UT, PRE 70, 025201(R) (2004); JCP 122, 224711 (2005)

Two-layer film: Mobilities, Energy

Matrix of mobility functions – symmetric, positive definite:

$$\mathbf{Q} = \frac{1}{6\mu_b}\begin{pmatrix} 2h_b^3 & 3h_b^2 h_t \\ 3h_b^2 h_t & 2\mu h_t^3 + 6 h_b h_t^2 \end{pmatrix}$$

Energy functional

$$F = \int_A \left[\frac{\gamma_1}{2}(\nabla h_b)^2 + \frac{\gamma_2}{2}(\nabla(h_b+h_t))^2 + f(h_b, h_t, h_b+h_t)\right] dA$$

Example: Local energy for van-der-Waals interactions

$$f(h_b, h_t, h_b+h_t) = -\frac{A_{gtbs}}{12\pi(h_b+h_t)^2} - \frac{A_{tbs}}{12\pi h_b^2} - \frac{A_{btg}}{12\pi h_t^2}$$

Dispersion relations - Nonlinear evolution - Rupture modes

Varicose mode — Zigzag mode — Mixed mode

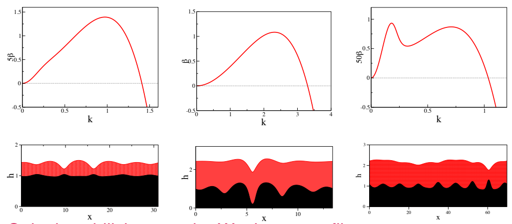

Only destabilizing van der Waals → film rupture → no long time evolution

Branch switching during coarsening

Time evolution — Stationary solutions

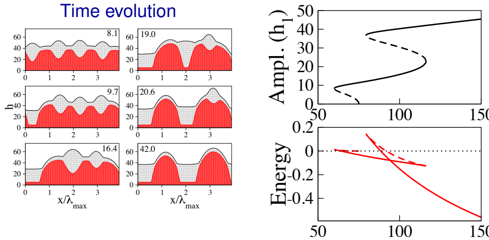

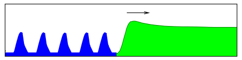

with L. Frastia, A.J. Archer, (H. Lopez)

Hydrodynamic equations in long-wave approximation I

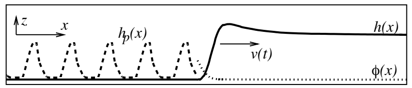

Film thickness evolution equation
[isothermal, without solute cf. Pismen 2002 [24,25], Thiele 2010 [26])

$$\partial_t h = -\nabla\cdot\mathbf{j}_{conv} - j_{evap} = \nabla\cdot[Q(h,\phi)\nabla p(h)] - \frac{\beta}{\rho}(p(h)-\mu\rho)$$

$$Q(h,\phi) = \frac{h^3}{3\eta(\phi)} \quad \text{mobility}$$

$$p(h) = -\gamma\Delta h - \Pi(h) \quad \text{pressure}$$

Hydrodynamic equations in long-wave approximation II

Evolution equation for effective 'layer thickness' $\psi = h\phi$
[see also Warner et al. 2003[27]]

$$\partial_t(\phi h) = -\nabla\cdot[\mathbf{j}_{\rm adv} + \mathbf{j}_{\rm diff}] = -\nabla\cdot[\phi\mathbf{j}_{\rm conv} + \mathbf{j}_{\rm diff}]$$
$$= \nabla\cdot[\phi Q(h,\phi)\nabla p(h)] + \nabla\cdot[D(\phi)h\nabla\phi]$$

Viscosity/diffusivity of dense suspension
[Quemada (1977)[28], Krieger-Doherty law, Einstein relation]

$$\eta(\phi) = \eta_0\left(1-\frac{\phi}{\phi_c}\right)^{-\nu} \qquad D(\phi) = \frac{k_BT}{6\pi r_0\eta(\phi)}$$

$\nu\ldots$ Literature gives various exponents below ≈ 2

Evolution equations account for solvent capillarity, wettability, evaporation, solute diffusion, nonlinear rheology

Basic morphologies and mechanisms

Final dried-in deposit (small system)

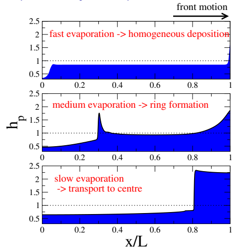

Pinning/depinning mechanism

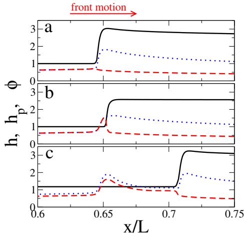

UT et al., J. Phys.-Cond. Mat. 21, 264016 (2009)

Pattern types – Examples

Dried-in deposition patterns close to "first ring"

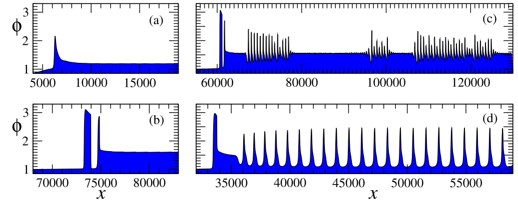

L. Frastia, A.J. Archer, UT, PRL 106, 077801 (2011);
Soft Matter 8, 11363 (2012)

Pattern types – morphological phase diagram

Depending on evaporation rate Ω and initial mean concentration ϕ_0

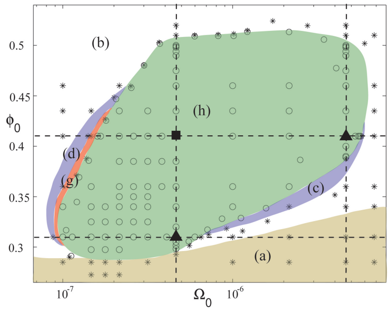

Line patterns – dependence on concentration

Deposit profiles and characteristics for $\Omega_0 = 4.64\times10^{-7}$

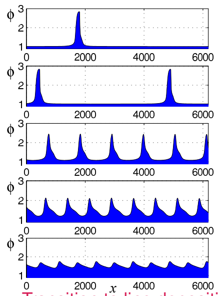

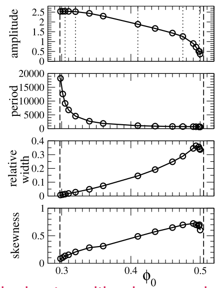

Transition to line deposition as depinning transition in comoving frame $\rightarrow$ depinning via Hopf and infinite period bifurcation

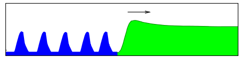

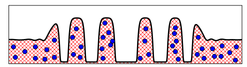

Reformulation and Extension

UT, EPJST 197, 213 (2011);
UT, A. Archer, M. Plapp, PoF **24**, 102107 (2012)

Diffusion equation as gradient dynamics

Evolution equation for conserved concentration

$$\partial_t\phi = \nabla\cdot\left\{Q(\phi)\nabla\frac{\delta F[\phi]}{\delta\phi}\right\}$$

with F only consisting of entropic contribution

$$F[h] = \int_V\left[\frac{kT}{a^3}\phi(\log\phi - 1)\right]dV$$

$Q(\phi) = \tilde{D}\phi\ldots$ mobility function ($\tilde{D}$ molecular mobility)

$$\partial_t\phi = \nabla\cdot\left[\tilde{D}\phi\nabla\left(\frac{kT}{a^3}\log\phi\right)\right] = \frac{\tilde{D}kT}{a^3}\Delta\phi = D\Delta\phi$$

Thermodynamic formulation of evolution equations for suspensions and solutions I

$$\partial_t h = \nabla\cdot\left[Q_{hh}\nabla\frac{\delta F}{\delta h} + Q_{h\psi}\nabla\frac{\delta F}{\delta\psi}\right] - Q_e\frac{\delta F}{\delta h}$$
$$\partial_t\psi = \nabla\cdot\left[Q_{\psi h}\nabla\frac{\delta F}{\delta h} + Q_{\psi\psi}\nabla\frac{\delta F}{\delta\psi}\right]$$

where $\psi = h\phi$ is the effective solute layer thickness

Evaporative flow – constant mobility

$$Q_e = \text{const} \geq 0$$

No contribution from $\delta F/\delta\psi$ to evaporation as ψ is conserved
$\longrightarrow$ Previous models miss osmotic pressure $(g - \phi g')$

Thermodynamic formulation of evolution equations II

Symmetric positive definite mobility matrix (cf. Onsager)

$$\mathbf{Q} = \begin{pmatrix} Q_{hh} & Q_{h\psi} \\ Q_{\psi h} & Q_{\psi\psi}\end{pmatrix} = \frac{1}{3\eta}\begin{pmatrix} h^3 & h^2\psi \\ h^2\psi & h\psi^2 + 3\tilde{D}\psi\end{pmatrix}$$

Free energy - extended interface Hamiltonian

$$F[h,\psi] = \int\left[\frac{\gamma}{2}(\nabla h)^2 + f(h) + h\,g\left(\frac{\psi}{h}\right)\right]dA.$$

At low concentrations only entropic contributions in ϕ

$$g(\phi) = \frac{k_BT}{a^3}\phi[\log(\phi) - 1] = \frac{k_BT}{a^3}\frac{\psi}{h}\left[\log\left(\frac{\psi}{h}\right) - 1\right]$$

Density-dependent transport coefficients

Viscosity of dense suspension (Quemada 1977, Krieger-Doherty law)

$$\eta(\phi) = \eta_0 \left(1 - \frac{\phi}{\phi_c}\right)^{-\nu}$$

$\nu \ldots$ Literature gives various exponents below ≈ 2

Solute mobility (related to 'Diffusion constant')
(Einstein relation valid for all densities)

$$\widetilde{Q}_{\psi\psi} = \frac{\widetilde{D}\psi}{\eta(\phi)} \quad \text{with} \quad \widetilde{D} = \frac{a^2}{6\pi} \quad \text{gives} \quad D(\phi) = \frac{k_B T}{6\pi a \eta(\phi)}$$

Extensions based on reformulation I

(i) Weakly interacting colloidal particles
no solute-solvent decomposition

Replace $g \sim \phi \log(\phi)$ by $g \sim \phi \log(\phi) - b\phi^2$

(ii) Strongly interactive colloidal particles
possible solute-solvent decomposition
Close to critical point (cf. Cahn-Hilliard double-well energy)

Use $g \sim \kappa(\nabla\phi)^2 + (\phi^2 - 1)^2$

Gives long-wave limit of model-H (as derived via asymptotics by Náraigh and Thiffeault (2010))

Extensions based on reformulation

(iii) Solute-dependent wettability

Replace $f(h)$ by $f(h,\phi)$

Convective and diffusive fluxes become:

$$\mathbf{J}_{\text{conv}} = Q_{hh}[\nabla(\gamma\Delta h - \partial_h f(h,\phi)) + \frac{1}{h}(\partial_\phi f(h,\phi))\nabla\phi]$$

$$\mathbf{J}_{\text{diff}} = -\tilde{D}\psi\nabla\left[\frac{1}{h}\partial_\phi f(h,\phi) + g'(\phi)\right]$$

New term: 'wettability equivalent' of Marangoni/Korteweg flow

UT, EPJST 197, 213-220 (2011); D. Todorova, submitted (2013)

Solute-dependent wettability - Hamaker constant

Film of solution

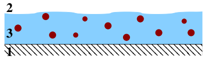

Homogenisation gives $\epsilon_3(\phi)$

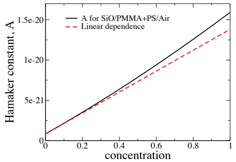

Hamaker 'constant'

$$A_{123}(\phi) = \frac{3k_bT}{4}\left(\frac{\epsilon_1 - \epsilon_3(\phi)}{\epsilon_1 + \epsilon_3(\phi)}\right)\left(\frac{\epsilon_2 - \epsilon_3(\phi)}{\epsilon_2 + \epsilon_3(\phi)}\right) + \frac{3h_p\nu_e}{8\sqrt{2}} \frac{(n_1^2 - n_3^2(\phi))(n_2^2 - n_3^2(\phi))}{\sqrt{(n_1^2 + n_3^2(\phi))(n_2^2 + n_3^2(\phi))}\left(\sqrt{n_1^2 + n_3^2(\phi)} + \sqrt{n_2^2 + n_3^2(\phi)}\right)}$$

ϕ – concentration of solute;
n_i – refractive indices;
ϵ_i – dielectric constants;
k_b – Boltzmann's constant;
T – temperature;
h_p – Planck's constant;
ν_e – main electronic absorption frequency.

Solute-dependent wettability - Film stability

Derjaguin pressure

$$\Pi(h) = -\frac{A(\phi)}{h^3} + \frac{B}{h^6}$$

$B > 0$ and $A_0 < 0$ (wetting)
⟶ pure solvent film absolutely stable

For $M_1 < 0$
⟶ pure solute film absolutely stable

No solute-solvent attraction (ideal gas-like solute)
⟶ no bulk solute-solvent decomposition

Linear stability diagram

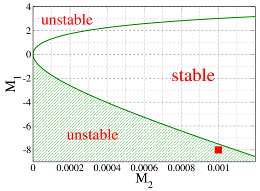

$h_0 = 15, \phi_0 = 0.2$

$$A(\phi) = |A_0|(-1 + M_1\phi)$$

$$M_2 = \frac{k_b T}{|A_0|}\frac{l^3}{a^3}$$

Solute-dependent wettability - Steady states

Solution family at $M_2 = 0.001$, $M_1 = -8$

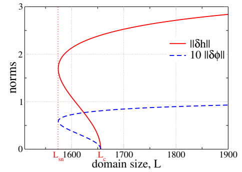

Drop/concentration profiles

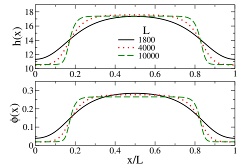

Coupling of film height and concentration degrees of freedom allows system to minimize energy further

Summary lecture 2

- Experiments with films/drops of mixtures/solutions/suspensions
- Gradient dynamics approach for two-layer films
- Gradient dynamics approach for mixtures (non-surface active)
- Selected results for two-layer films, line deposition and dewtting mixtures

Depinning transitions and deposition patterns

Uwe Thiele

Cambridge, July 2013

ITN MULTIFLOW

Loughborough University

Contact line pinning, contact angle hysteresis and stick-slip motion

Dussan (1979)[29]
Contact angle hysteresis

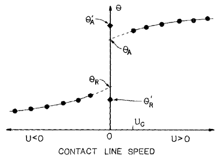

Schäffer and Wong (1998)[7]
Stick-slip motion

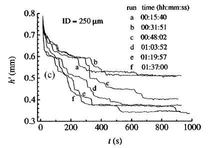

Depinning of drop on striped substrate

Varagnolo et al., arXiv (2013)

Stick-slipping drop

Mean drop velocity

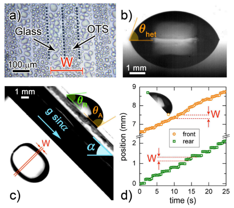

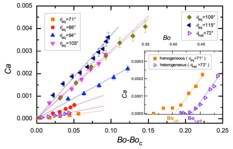

How can the depinning transition be characterized?

The coffee stain effect

R.D. Deegan (1997-2000)[30–32]
(Polystyrene micro-spheres in water)

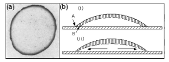

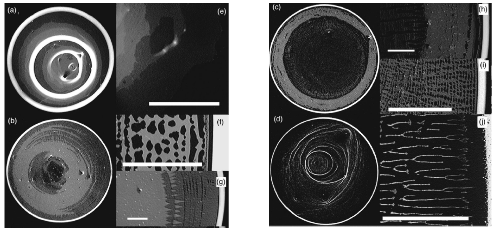

Volume fractions (a) 1%, (b) 0.25%, (c) 0.13%, and (d) 0.063%

Dewetting evaporating suspensions – line patterns

Zhiqun Lin et al. (2006-2008)[21,33–35]
(CdSe/ZnS core/shell, 4.4nm (right) and 5.5nm (left) in diameter, in toluene)

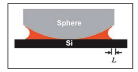

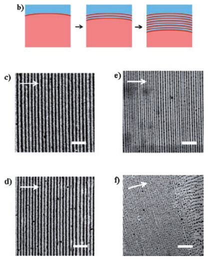

Concentrations: 0.25mg/ml, 0.15mg/ml, 0.05mg/ml, 0.05mg/ml

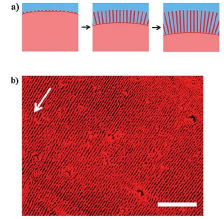

Concentration: 0.25mg/ml

Dewetting evaporating polymer solutions

Yabu & Shimomura (2005)[36]
(Polystyrene in chloroform)

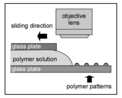

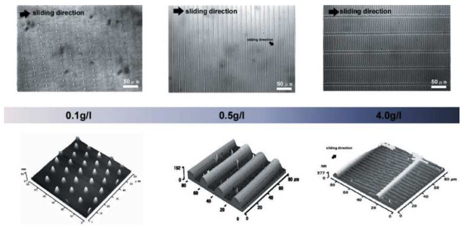

Patterning by Langmuir-Blodgett transfer

Chi, Fuchs et al (2004) – Transfer of DPPC onto silicon oxide[23]

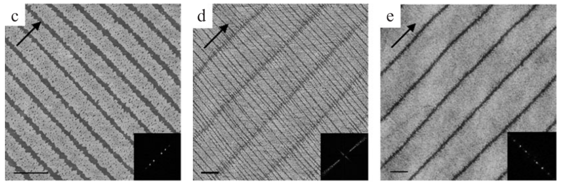

SFM images, bar 2μm

see also Riegler et al 1992/94[37,38]

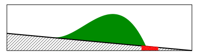

with E Knobloch (2d/3d), P Beltrame (3d), P Hänggi (3d)

Driven drops/film on heterogeneous substrate

Film thickness evolution equation in long-wave approximation

$$\partial_t h = -\nabla\cdot\left\{\frac{h^3}{3\eta}\nabla\left[\gamma\Delta h + \Pi(h,\mathbf{r})\right] + \mu\mathbf{e_x}\right\}$$

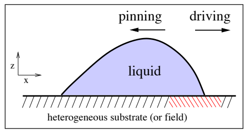

Non-dimensional parameters

$\bar{h}\ldots$ mean film thickness
$L_x \times L_y \ldots$ system size / period
$\mu\ldots$ driving force

Note: Very similar equation describes drops on a rotating cylinder $\rightarrow$ expect similar transitions

Periodic array of local wettability defect

Wettability via Derjaguin (disjoining) pressure

$$\Pi(h,\mathbf{r}) = \kappa\left(\frac{b}{h^3} - [1+\epsilon\xi(x)]\,e^{-h}\right)$$

$$\xi(x) = 2\,\{\mathrm{cn}[2K(k)x/L,k]\}^2 - \Delta$$

$K(k)\ldots$ complete elliptic integral of the first kind
$\Delta\ldots$ shift to have $\int\xi(x)dx = 0$

Further parameters

- $\epsilon\ldots$ wettability contrast
  - $\epsilon < 0$ hydrophilic defect
  - $\epsilon > 0$ hydrophobic defect
- $s \equiv -\log(1-k)\ldots$ steepness of defect

Profiles of pinned driven 2d drops (3d transversally invariant ridges)

Hydrophilic defect

Hydrophobic defect

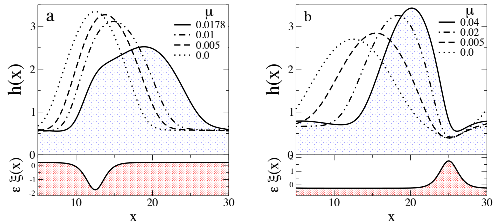

Focus on small amplitude drops to resolve details of bifurcational structure

Dynamics of depinning of a 2d drop pinned by a hydrophilic defect

Depinning via sniper bifurcation – Stick-slip infinitely slow at transition.

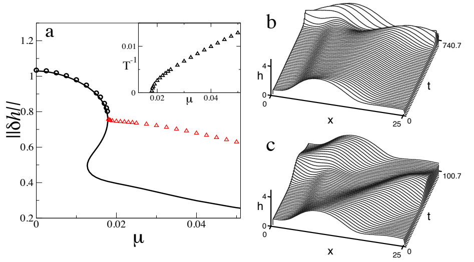

UT and E. Knobloch: PRL 97, 204501 (2006); NJP 8, 313 (2006)

Drop depinning from hydrophilic line defect via SNIPer bifurcation

Bifurcation diagram

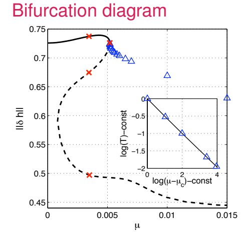

Steady drops

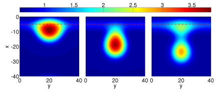

Time evolution

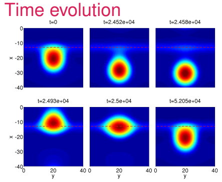

P. Beltrame, P. Hänggi, UT; EPL 86, 24006 (2009)
(cf. UT and E. Knobloch: PRL 97, 204501 (2006); NJP 8, 313 (2006)

Stationary and dynamic states in 3d – Multistability

Complete picture has to relate

- Depinning transitions of 3d drops and transversally invariant ridges (2d drops)
- Plateau-Rayleigh instability of a ridge (zero/finite driving with/without heterogeneity
- Rivulet solutions and their stability w.r.t. surface waves with/without heterogeneity

Depinnning of large contact angle drops

Description by Stokes equation
with D. Herde, M. Brinkmann and S. Herminghaus

- Space-dependent microscopic contact angle imposed
- steady drops (continuation steady Stokes equation, minimisation energy)
- slip-length controlled sliding drops
- large contact angles (45^o, 90^o)

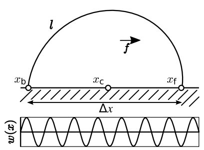

Large contact angle drops - sliding drops

Dependence of onset of sliding on slip length

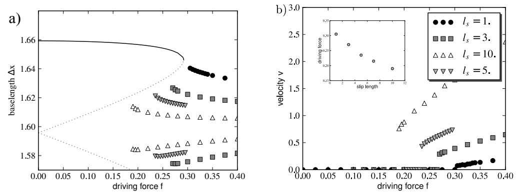

With increasing slip length the (homoclinic) depinning bifurcation occurs at smaller driving
Less dissipation at same drop speed→ More energy stored as interfacial energy (and then used to overcome hydrophobic patch)

D. Herde, UT, S. Herminghaus, M. Brinkmann EPL 100, 16002 (2012)

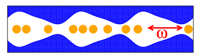

with A. Pototsky, A. J. Archer, S.E. Savel'ev, and F. Marchesoni

DDFT evolution equation as gradient dynamics

Evolution equation for conserved density $\rho(x,t)$

$$\partial_t \rho = \partial_x \left\{ Q(\rho)\, \partial_x \frac{\delta F[\rho]}{\delta \rho} \right\}$$

with free energy

$$F[\rho] = T \int_{-\frac{S}{2}}^{\frac{S}{2}} dx\, \rho[\ln\rho - 1] + \int_{-\frac{S}{2}}^{\frac{S}{2}} dx\, U_{\rm eff}(x)\rho + F_{\rm at}[\rho] + F_{\rm hc}[\rho]$$

$Q(\rho) = \rho \ldots$ mobility
$U_{\rm eff}(x) \ldots$ external potential (here independent of time)
$F_{\rm at}[\rho] \ldots$ attractive interaction
$F_{\rm hc}[\rho] \ldots$ hard-core repulsive interaction

Contributions to energy

External potential (periodic part & overall tilt)

$$U_{\rm eff}(x) = U(x) - Ax \qquad U(x) = \sin(2\pi x) + 0.25\sin(4\pi x)$$

Attractive interaction

$$F_{\rm at}[\rho] = \int_{-\frac{S}{2}}^{\frac{S}{2}} dx \int_{x-\frac{S}{2}}^{x+\frac{S}{2}} dx'\, w_{\rm at}(|x-x'|)\frac{\rho(x)\rho(x')}{2} \quad \text{with} \quad w_{\rm at}(x) = -\alpha e^{-\lambda x}$$

Hard-core repulsion

$$F_{\rm hc}[\rho] = \frac{1}{2}\int_{-\frac{S}{2}}^{\frac{S}{2}} dx\, \phi[\rho(x)] \left\{ \rho\left(x + \frac{h}{2}\right) + \rho\left(x - \frac{h}{2}\right) \right\}$$

where $\phi[\rho] = -T\ln[1-\eta]$ and $\eta(x,t) = \int_{x-h/2}^{x+h/2} dx'\, \rho(x',t)$

Depinning transition for point particles ($h = 0$)

Bifurcation diagram for $S = 3L$ domain

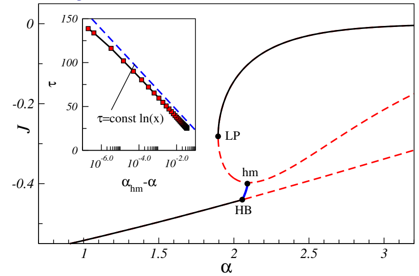

$\alpha \ldots$ interaction strength ($\sim$ increasing contact angle)
driving: $A = -1$, interaction length $\lambda = 5$

Depinned state for 3L domain - movie

Motion via volume mode

driving: $A = -1$, interaction length $\lambda = 5$ and strength $\alpha = 2.09$

Influence of size of rod-like particles ($h > 0$)

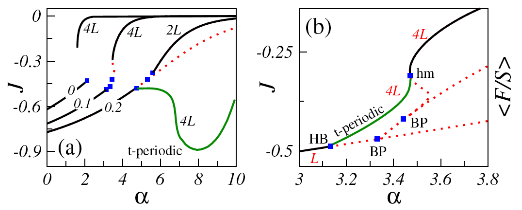

driving: $A = -1$, interaction length $\lambda = 5$, domain size $S = 4L$

A. Pototsky, A. J. Archer, S.E. Savel'ev, UT and F. Marchesoni, PRE 83, 061401 (2011)

Depinned 'frozen' clusters - movie

Driving: $A = -1$, particle size $h = 0.2$, interaction strength

Depinned 'frozen' clusters - snapshot

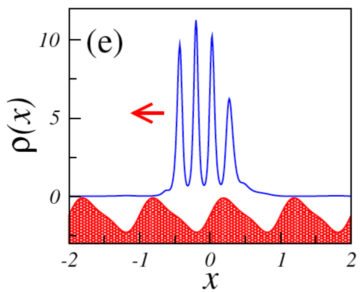

Driving: $A = -1$, particle size $h = 0.2$, interaction strength $\alpha = 7.5$, interaction length $\lambda = 5$

Conclusions for depinning drops / density distributions

Depinning drops/ridges in 2d/3d

- Drops/ridges may depin via sniper/Hopf/homoclinic bifurcation
- Stick-slip motion beyond depinning (sniper/homoclinic), related to translation mode
- Intricate 3d behaviour (coupling to Plateau-Rayleigh instability)

DDFT for interacting particles in modulated nano-pore

- Interplay of steady-state (pitchfork) and depinning transitions (Hopf/homoclinic) [picture not yet complete]
- Depinning dynamics via volume transfer *or* translation mode

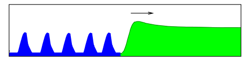

with L. Frastia, A.J. Archer, (H. Lopez)

Pattern types – morphological phase diagram

Depending on evaporation rate Ω and initial mean concentration ϕ_0

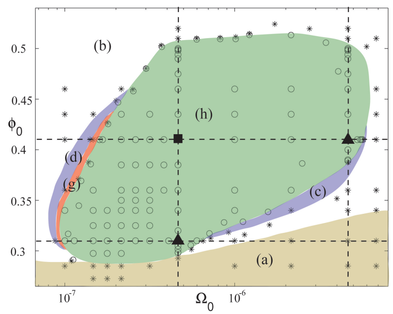

Line patterns – dependence on concentration

Deposit profiles and characteristics for $\Omega_0 = 4.64 \times 10^{-7}$

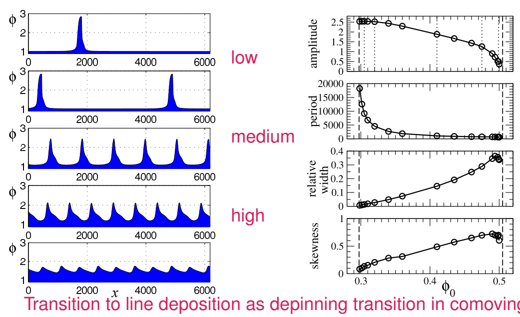

Transition to line deposition as depinning transition in comoving frame → depinning via Hopf and infinite period bifurcation

LANGMUIR-BLODGETT TRANSFER

Thin film model by Köpf, Gurevich, Friedrich, and Chi (2010)[39]

Geometry

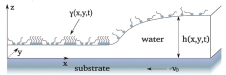

Resulting line patterns

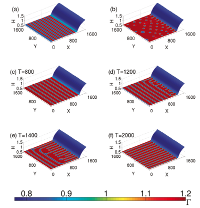

Evolution equations

$$\partial_t \Gamma = -\nabla \cdot \left[\frac{\Gamma h^2}{2} \nabla p + \Gamma h \nabla \Sigma - V \Gamma \right]$$

$$\partial_t h = -\nabla \cdot \left[\frac{h^3}{3} \nabla p + \frac{h^2}{2} \nabla \Sigma - V h \right] - \Omega \mu(h, \Gamma)$$

Special case of gradient dynamics model for insoluble surfactants
*UT, A. Archer, M. Plapp, PoF **24**, 102107 (2012)*

Reduced description with Cahn-Hilliard-type model

Observations with full model

- Patterning rather insensitive to details of BC at meniscus side and details of evaporation
- Phase transition triggered by strong decrease of film height in contact region
- ⟶ One may 'fix' film profile and incorporate as heterogeneous medium into simple model for phase separation

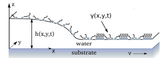

Cahn-Hilliard model with dragging term

$$\partial_t c = -\Delta[\Delta c - c^3 + (1 - \mu\zeta(\boldsymbol{x}))\, c] - \boldsymbol{V} \cdot \nabla c \qquad \text{with} \qquad \boldsymbol{V} = (V, 0)$$

and space dependent external field (smooth step)

$$\zeta(\boldsymbol{x}) = \zeta(x) = -\frac{1}{2}\left[1 + \tanh\left(\frac{x - x_s}{l_s}\right)\right]$$

Reduced model (Cahn-Hilliard-type) - Results

Depinning bifurcation diagram

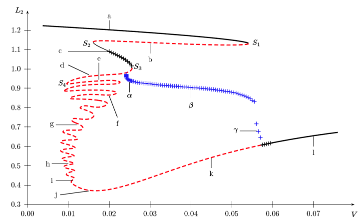

Steady profiles

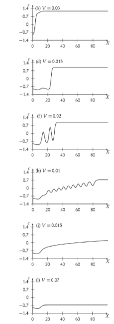

Homoclinic (low V) and Hopf (high V) bifurcation
Heteroclinic snaking of localised (front) states

M. Köpf, S. Gurevich, R. Friedrich, UT, New J. Phys. 14, 023016 (2012)

Summary lecture 3

- Experiments with depinning drops and line deposition
- Bifurcation study for depinning drops
- DDFT approach for nano-particles in heterogeneous pore (depinning transitions)
- Selected results for line deposition

General outlook

Gradient dynamics forms of evolution equations

- Understand full spectrum of two-field models better
- Use to develop new models
- Strongly/weakly anchored nematic liquid crystals
- Evaporation models (including osmotic pressure)
- Formulation for soluble surfactants
- Driven systems? Which? Potential energy!
- Further explore relation to DDFT

Depinning transitions

- How do they emerge?
- How are the different systems related?
- Simplified models?

References I

[1] G. Reiter. Dewetting of thin polymer films. *Phys. Rev. Lett.*, 68:75–78, 1992. doi: 10.1103/PhysRevLett.68.75.

[2] G. Reiter. Unstable thin polymer films: Rupture and dewetting processes. *Langmuir*, 9:1344–1351, 1993. doi: 10.1021/la00029a031.

[3] A. Sharma and G. Reiter. Instability of thin polymer films on coated substrates: Rupture, dewetting and drop formation. *J. Colloid Interface Sci.*, 178:383–399, 1996. doi: 10.1006/jcis.1996.0133.

[4] J. Becker, G. Grün, R. Seemann, H. Mantz, K. Jacobs, K. R. Mecke, and R. Blossey. Complex dewetting scenarios captured by thin-film models. *Nat. Mater.*, 2:59–63, 2003.

[5] Z. Lin, T. Kerle, T. P. Russell, E. Schäffer, and U. Steiner. Structure formation at the interface of liquid-liquid bilayer in electric field. *Macromolecules*, 35:3971–3976, 2002.

[6] T. Podgorski, J.-M. Flesselles, and L. Limat. Corners, cusps, and pearls in running drops. *Phys. Rev. Lett.*, 87: 036102, 2001. doi: 10.1103/PhysRevLett.87.036102.

[7] E. Schäffer and P. Z. Wong. Dynamics of contact line pinning in capillary rise and fall. *Phys. Rev. Lett.*, 80: 3069–3072, 1998. doi: 10.1103/PhysRevLett.80.3069.

[8] G. Reiter and A. Sharma. Auto-optimization of dewetting rates by rim instabilities in slipping polymer films. *Phys. Rev. Lett.*, 87:166103, 2001. doi: 10.1103/PhysRevLett.87.166103.

[9] I. Veretennikov, A. Indeikina, and H.-C. Chang. Front dynamics and fingering of a driven contact line. *J. Fluid Mech.*, 373:81–110, 1998.

[10] D van Effenterre, MP Valignat, and D Roux. Coupling between the nematic/isotropic transition and a thickness transition: A theoretical approach. *Europhys. Lett.*, 62:526–532, 2003.

[11] J. Q. Carou, N. J. Mottram, S. K. Wilson, and B. R. Duffy. A mathematical model for blade coating of a nematic liquid crystal. *Liq. Cryst.*, 34:621–631, 2007.

[12] M. Ben Amar and L. J. Cummings. Fingering instabilities in driven thin nematic films. *Phys. Fluids*, 13: 1160–1166, 2001.

[13] M. Geoghegan and G. Krausch. Wetting at polymer surfaces and interfaces. *Prog. Polym. Sci.*, 28:261–302, 2003. doi: 10.1016/S0079-6700(02)00080-1.

References II

[14] A. Faldi, R. J. Composto, and K. I. Winey. Unstable polymer bilayers. 1. Morphology of dewetting. *Langmuir*, 11:4855, 1995.

[15] H. Wang and R. J. Composto. Wetting and phase separation in polymer blend films: Identification of four thickness regimes with distinct morphological pathways. *Interface Sci.*, 11:237–248, 2003.

[16] P. Müller-Buschbaum, E. Bauer, S. Pfister, S. V. Roth, M. Burghammer, C. Riekel, C. David, and U. Thiele. Creation of multi-scale stripe-like patterns in thin polymer blend films. *Europhys. Lett.*, 73:35–41, 2006. doi: 10.1209/epl/i2005-10369-6.

[17] E. Pauliac-Vaujour, A. Stannard, C. P. Martin, M. O. Blunt, I. Notingher, P. J. Moriarty, I. Vancea, and U. Thiele. Fingering instabilities in dewetting nanofluids. *Phys. Rev. Lett.*, 100:176102, 2008. doi: 10.1103/PhysRevLett.100.176102.

[18] U. Thiele. *Entnetzung von Kollagenfilmen.* PhD thesis, Technische Universität Dresden, 1998.

[19] X. Gu, D. Raghavan, J. F. Douglas, and A. Karim. Hole-growth instability in the dewetting of evaporating polymer solution films. *J. Polym. Sci. Pt. B-Polym. Phys.*, 40:2825–2832, 2002.

[20] I. Vancea, U. Thiele, E. Pauliac-Vaujour, A. Stannard, C. P. Martin, M. O. Blunt, and P. J. Moriarty. Front instabilities in evaporatively dewetting nanofluids. *Phys. Rev. E*, 78:041601, 2008. doi: 10.1103/PhysRevE.78.041601.

[21] J. Xu, J. F. Xia, and Z. Q. Lin. Evaporation-induced self-assembly of nanoparticles from a sphere-on-flat geometry. *Angew. Chem.-Int. Edit.*, 46:1860–1863, 2007. doi: 10.1002/anie.200604540.

[22] K. Spratte, L. F. Chi, and H. Riegler. Physisorption instabilities during dynamic Langmuir wetting. *Europhys. Lett.*, 25:211–217, 1994.

[23] S. Lenhert, L. Zhang, J. Mueller, H. P. Wiesmann, G. Erker, H. Fuchs, and L. F. Chi. Self-organized complex patterning: Langmuir-Blodgett lithography. *Adv. Mater.*, 16:619–624, 2004. doi: 10.1002/adma.200306203.

[24] A. V. Lyushnin, A. A. Golovin, and L. M. Pismen. Fingering instability of thin evaporating liquid films. *Phys. Rev. E*, 65:021602, 2002. doi: 10.1103/PhysRevE.65.021602.

[25] L. M. Pismen. Mesoscopic hydrodynamics of contact line motion. *Colloid Surf. A-Physicochem. Eng. Asp.*, 206:11–30, 2002. doi: 10.1016/S0927-7757(02)00059-6.

References III

[26] U. Thiele. Thin film evolution equations from (evaporating) dewetting liquid layers to epitaxial growth. *J. Phys.: Condens. Matter*, 22:084019, 2010. doi: 10.1088/0953-8984/22/8/084019.

[27] M. R. E. Warner, R. V. Craster, and O. K. Matar. Surface patterning via evaporation of ultrathin films containing nanoparticles. *J. Colloid Interface Sci.*, 267:92–110, 2003. doi: 10.1016/S0021-9797(03)00640-4.

[28] D. Quemada. Rheology of concentrated disperse systems and minimum energy-dissipation principle I. Viscosity-concentration relationship. *Rheol. Acta*, 16:82–94, 1977. doi: 10.1007/BF01516932.

[29] E. B. Dussan. On the spreading of liquids on solid surfaces: Static and dynamic contact lines. *Ann. Rev. Fluid Mech.*, 11:371–400, 1979. doi: 10.1146/annurev.fl.11.010179.002103.

[30] R. D. Deegan, O. Bakajin, T. F. Dupont, G. Huber, S. R. Nagel, and T. A. Witten. Capillary flow as the cause of ring stains from dried liquid drops. *Nature*, 389:827–829, 1997. doi: 10.1038/39827.

[31] R. D. Deegan. Pattern formation in drying drops. *Phys. Rev. E*, 61:475–485, 2000. doi: 10.1103/PhysRevE.61.475.

[32] R. D. Deegan, O. Bakajin, T. F. Dupont, G. Huber, S. R. Nagel, and T. A. Witten. Contact line deposits in an evaporating drop. *Phys. Rev. E*, 62:756–765, 2000. doi: 10.1103/PhysRevE.62.756.

[33] J. Xu, J. F. Xia, S. W. Hong, Z. Q. Lin, F. Qiu, and Y. L. Yang. Self-assembly of gradient concentric rings via solvent evaporation from a capillary bridge. *Phys. Rev. Lett.*, 96:066104, 2006. doi: 10.1103/PhysRevLett.96.066104.

[34] S. W. Hong, J. F. Xia, and Z. Q. Lin. Spontaneous formation of mesoscale polymer patterns in an evaporating bound solution. *Adv. Mater.*, 19:1413–1417, 2007. doi: 10.1002/adma.200601882.

[35] S. W. Hong, W. Jeong, H. Ko, M. R. Kessler, V. V. Tsukruk, and Z. Q. Lin. Directed self-assembly of gradient concentric carbon nanotube rings. *Adv. Funct. Mater.*, 18:2114–2122, 2008. doi: 10.1002/adfm.200800135.

[36] H. Yabu and M. Shimomura. Preparation of self-organized mesoscale polymer patterns on a solid substrate: Continuous pattern formation from a receding meniscus. *Adv. Funct. Mater.*, 15:575–581, 2005. doi: 10.1002/adfm.200400315.

[37] H. Riegler and K. Spratte. Structural-changes in lipid monolayers during the Langmuir-Blodgett transfer due to substrate monolayer interactions. *Thin Solid Films*, 210:9–12, 1992. doi: 10.1016/0040-6090(92)90153-3.

References IV

[38] K. Spratte and H. Riegler. Steady-state morphology and composition of mixed monomolecular films (Langmuir monolayers) at the air/water interface in the vicinity of the 3-phase line - model-calculations and experiments. *Langmuir*, 10:3161–3173, 1994.

[39] M. H. Köpf, S. V. Gurevich, R. Friedrich, and L. F. Chi. Pattern formation in monolayer transfer systems with substrate-mediated condensation. *Langmuir*, 26:10444–10447, 2010. doi: 10.1021/la101900z.